



Efficient Generation of Myelinating Oligodendrocytes from Primary Progressive Multiple Sclerosis Patients by Induced Pluripotent Stem Cells

Panagiotis Douvaras,¹ Jing Wang,² Matthew Zimmer,¹ Stephanie Hanchuk,¹ Melanie A. O'Bara,² Saud Sadiq,³ Fraser J. Sim,² James Goldman,⁴ and Valentina Fossati^{1,*}

¹The New York Stem Cell Foundation Research Institute, New York, NY 10032, USA

²Department of Pharmacology and Toxicology, School of Medicine and Biomedical Sciences, University at Buffalo, Buffalo, NY 14214, USA

³Tisch Multiple Sclerosis Research Center of New York, New York, NY 10019, USA

⁴Department of Pathology and Cell Biology, Columbia University, New York, NY 10032, USA

*Correspondence: vfossati@nyscf.org

<http://dx.doi.org/10.1016/j.stemcr.2014.06.012>

This is an open access article under the CC BY-NC-ND license (<http://creativecommons.org/licenses/by-nc-nd/3.0/>).

SUMMARY

Multiple sclerosis (MS) is a chronic demyelinating disease of unknown etiology that affects the CNS. While current therapies are primarily directed against the immune system, the new challenge is to address progressive MS with remyelinating and neuroprotective strategies. Here, we develop a highly reproducible protocol to efficiently derive oligodendrocyte progenitor cells (OPCs) and mature oligodendrocytes from induced pluripotent stem cells (iPSCs). Key elements of our protocol include adherent cultures, dual SMAD inhibition, and addition of retinoids from the beginning of differentiation, which lead to increased yields of OLIG2 progenitors and high numbers of OPCs within 75 days. Furthermore, we show the generation of viral and integration-free iPSCs from primary progressive MS (PPMS) patients and their efficient differentiation to oligodendrocytes. PPMS OPCs are functional, as demonstrated by *in vivo* myelination in the shiverer mouse. These results provide encouraging advances toward the development of autologous cell therapies using iPSCs.

INTRODUCTION

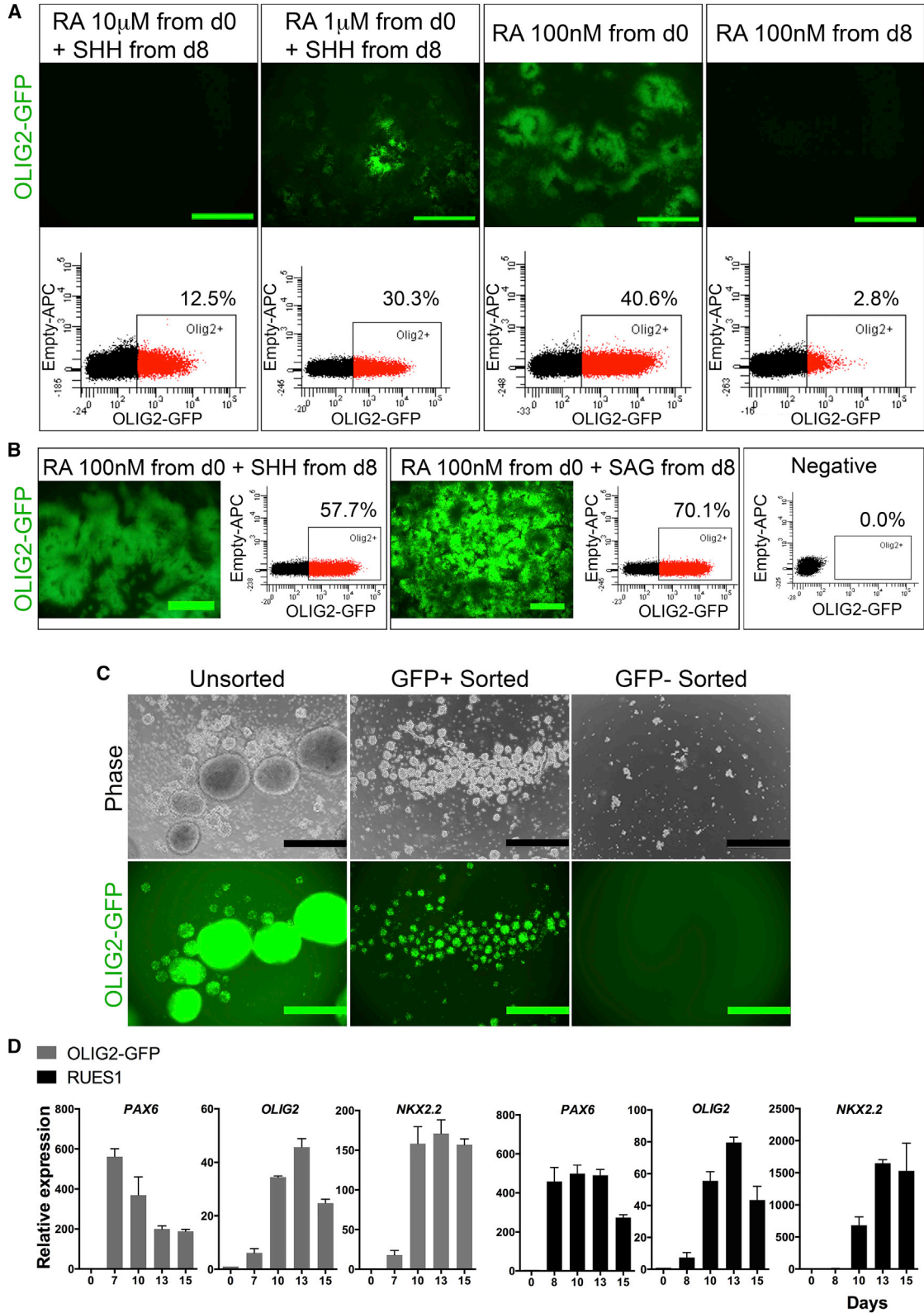
Multiple sclerosis (MS) is a chronic, inflammatory, demyelinating disease of the CNS that is distinguished by recurrent episodes of focal inflammatory demyelination and consequent neurological symptoms (relapsing remitting MS [RRMS]). Although relapses usually resolve in spontaneous remission, RRMS can evolve with time into a secondary progressive form characterized by irreversible accumulation of disabilities. Furthermore, patients affected by the most severe primary progressive form (PPMS) experience a steady neurological decline from the onset of the disease (Antel et al., 2012). Currently available treatments targeting the immune system are highly effective at reducing or even stopping the intermittent episodes of inflammation, but they do not influence the course of progressive MS. Therapeutic options for PPMS patients are limited to symptomatic treatments and the long-term prognosis is generally poor (Rice et al., 2013). Clearly, the unsolved challenge in the MS field is to develop neuroprotective and remyelinating strategies for the treatment of progressive MS patients (Hauser et al., 2013). The generation of patient-specific cells from induced pluripotent stem cells (iPSCs) or somatic cell nuclear transfer has recently emerged as a promising strategy for the development of autologous cell therapies (Goldman et al., 2012; Yamada et al., 2014). iPSC-derived oligodendrocyte progenitor cells (OPCs) were shown to successfully remyelinate and rescue a hypomyelinated mouse model, raising the possibility of future clinical trials (Wang et al., 2013).

However, oligodendrocyte differentiation protocols are still inefficient and require over 120 days in culture. Therefore, an improved protocol that can generate large numbers of purified OPCs in a relatively short time is highly desirable. Moreover, this protocol should be reproducible and highly efficient among different iPSC lines, including those derived from MS patients. We have pioneered the efficient and robust generation of iPSC-derived OPCs from PPMS patients. Our protocol recapitulates the major steps of oligodendrocyte differentiation from neural stem cells to OLIG2⁺ progenitors and finally to O4⁺ OPCs in a significantly shorter time than the 120–150 days required by the most recently published protocols (Wang et al., 2013; Stacpoole et al., 2013). Furthermore, O4⁺ OPCs were able to differentiate into MBP⁺ mature oligodendrocytes *in vitro* and to myelinate axons *in vivo* when injected into immunocompromised shiverer (*shi/shi*) mice. No abnormal growths were observed. Our results provide a proof of concept that transplantation of iPSC-derived, patient-specific cells for remyelination is technically feasible.

RESULTS

Retinoic Acid Is Critical for Efficient Differentiation of iPSCs to Oligodendrocytes

We aimed to develop an efficient differentiation protocol that recapitulates the critical developmental stages of oligodendrocyte specification as it occurs in the spinal cord. In this process, PAX6⁺ neural stem cells give rise to OLIG2⁺



(legend on next page)



Stem Cell Reports

iPSC-Derived Oligodendrocytes from MS Patients

progenitors, which become committed to the oligodendrocyte lineage by coexpressing NKX2.2 (pre-OPCs). They then differentiate to early OPCs by upregulating SOX10 and PDGFR α , followed by late OPCs expressing the sulfated glycolipid antigen recognized by the O4 antibody, and finally mature to myelin basic protein (MBP)⁺ oligodendrocytes (Hu et al., 2009a). We utilized an OLIG2-GFP knockin human embryonic stem cell (hESC) reporter line to track the OLIG2⁺ progenitors by live fluorescent imaging (Liu et al., 2011). First, we induced PAX6⁺ cells using dual inhibition of SMAD signaling in adherent cultures (Chambers et al., 2009). Next, to mimic the embryonic spinal cord environment, we applied different concentrations of retinoic acid (RA) and/or sonic hedgehog (SHH) at various times and quantified the OLIG2-GFP expression by flow cytometry (Figure 1A). Application of 100 nM RA from the beginning of induction generated 40.6% of OLIG2⁺ progenitors, whereas addition of SHH at 100 ng/ml from day 8 increased the yield to 57.7% (Figure 1B). Interestingly, cells without exogenous SHH during the first 12 days showed an upregulation of SHH mRNA (Figure S1A available online) and differentiated to O4⁺ cells, although at a lower efficiency compared with cells treated with SHH (Figure S1B). We then replaced the recombinant human SHH protein with the smoothed agonist (SAG), which increased the yield further to 70.1% OLIG2⁺ progenitors (Figure 1B). At day 12, cells were detached for sphere aggregation. The minimum number of cells required to form a sphere was 100, and we noted that the majority of the cells in the spheres were GFP⁺. To investigate this further, we sorted d12 cultures for GFP and observed that only GFP⁺ cells formed aggregates, whereas the GFP⁻ population did not (Figure 1C). This suggests that the aggregation step alone provides enrichment for the OLIG2⁺ population.

Next, we validated the initial steps toward the generation of OLIG2⁺ progenitors by differentiating a second hESC line (RUES1) and comparing the transcript levels of PAX6, OLIG2, and NKX2.2 by quantitative RT-PCR (qRT-PCR). The upregulation of these transcription factors followed a temporal pattern similar to that of the OLIG2-GFP line, with PAX6 induction around day 7, OLIG2 peak around day 13, and sustainably high levels of NKX2.2 after day

10 (Figure 1D). Based on these results, we used the nongenetically modified RUES1 line to develop the following steps of the protocol from OLIG2⁺ progenitors to MBP⁺ mature oligodendrocytes (Figure 2A). PAX6⁺ cells arose at day 7, and by day 12 they were arranged into multilayered structures (Figures 2B and 2C). From day 12 to day 30 the cells were grown as spheres, and they were then plated onto poly-L-ornithine/laminin-coated dishes for the remainder of the differentiation protocol.

To promote maturation toward the O4⁺ stage, platelet-derived growth factor AA (PDGF-AA), hepatocyte growth factor (HGF), insulin-like growth factor 1 (IGF1), and neurotrophin 3 (NT3) were added to the culture medium from day 20 onward. OLIG2⁺ progenitors upregulated NKX2.2 (pre-OPCs) and then SOX10 (early OPCs), and they finally matured to late OPCs, which were identified by O4 live staining and by their highly ramified processes (Figures 2D–2G). O4⁺ OPCs expressing OLIG2, SOX10, and NG2 (Figures 2H–2J) appeared as early as day 50 and increased dramatically around day 75. During the differentiation, 40%–50% of progenitor cells were proliferative, as indicated by Ki67 staining. However, the highly ramified O4⁺ cells did not divide in vitro (Figures S2A–S2C). Additionally, 34% \pm 4% of O4⁺ OPCs differentiated into MBP⁺ mature oligodendrocytes after growth-factor withdrawal from the medium for at least 3 weeks (Figures 2K, 2L, and S2D). Our cultures also consisted of other cell types (15% \pm 2% GFAP⁺ astrocytes and 20% \pm 2% MAP2⁺ neurons of total cells, respectively; Figures 2M and S2E).

Oligodendrocytes Can Be Efficiently Generated from PPMS-iPSC Lines

To determine whether this protocol could be applied to iPSC lines from subjects with PPMS, we obtained skin biopsies from four PPMS patients. Fibroblast cultures were established from the biopsies and iPSCs were generated using a cocktail of modified mRNAs (Warren et al., 2010) together with a cluster of miRNAs to improve the reprogramming efficiency (StemGent). From day 12 to day 15 of reprogramming, TRA-1-60⁺ colonies (Figure S3A), identified by live staining, were picked, expanded, and characterized by immunofluorescence for pluripotency markers (Figure S3B).

Figure 1. RA and SHH Requirement to Derive OLIG2⁺ Progenitor Cells

- (A) Live imaging and flow-cytometric quantification of OLIG2-GFP cells at day 14 of differentiation under different conditions for RA and SHH.
- (B) Comparison between the addition of SHH or SAG at day 8 and the best RA condition via live imaging and FACS analysis. Negative: hESC line RUES1.
- (C) Assessment of sphere formation for unsorted or sorted GFP⁺ and GFP⁻ cells.
- (D) Temporal gene-expression profile for PAX6, OLIG2, and NKX2.2 under optimal RA and SHH conditions. Error bars are SEM (n = 3 independent experiments). Scale bars represent 500 μ m.
- See Figure S1 for further optimizations of RA and SHH.

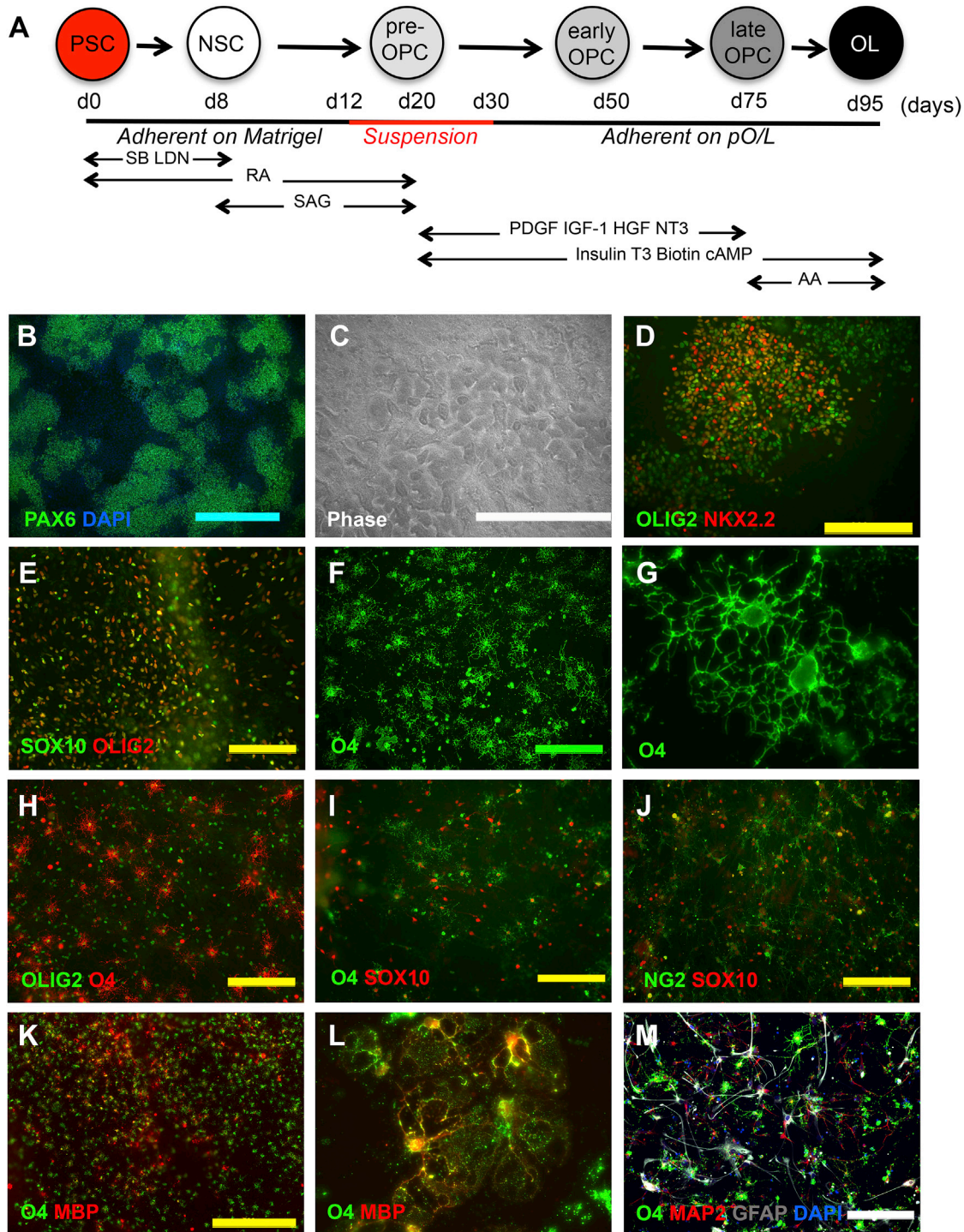


Figure 2. Generation of Oligodendrocytes from Human PSCs

(A) Diagram of the protocol for differentiation from hPSCs to mature oligodendrocytes.

(B–M) Sequential steps of in vitro oligodendrocyte differentiation of RUES1 cells, showing PAX6⁺ neural stem cells at day 8 (B), phase contrast of the multilayered structures at day 12 (C), OLIG2⁺NKX2.2⁺ pre-OPCs at day 18 (D), SOX10⁺OLIG2⁺ early OPCs (E), live imaging of O4⁺ late OPCs (F), a cropped image of O4⁺ cells to highlight the ramified processes (G), O4⁺ OPCs coexpressing OLIG2 (H), O4⁺ OPCs coexpressing SOX10 (I), sorted O4⁺ OPCs coexpressing SOX10 and NG2 (J), terminally differentiated MBP⁺ oligodendrocytes at low (K) and

(legend continued on next page)



Stem Cell Reports

iPSC-Derived Oligodendrocytes from MS Patients

Expression profiling for seven pluripotency genes confirmed that all four iPSC lines exhibited a profile comparable to that of a reference hESC line and divergent from the parental fibroblasts (Figure S3C). All iPSC lines displayed a normal karyotype (Figure S3D) and were able to differentiate into cell types of the three germ layers, both in vitro via spontaneous embryoid body differentiation (Figure S3E) and in vivo via teratoma assay (Figure S3F).

Next, we assessed whether the oligodendrocyte differentiation protocol was reproducible with our PPMS-iPSC lines. All iPSC lines tested were found to perform similarly to the RUES1 line (Figures 3A–3I). The protocol was greatly reproducible and highly efficient as calculated by the frequency of sorted O4⁺ OPCs, with up to 70% O4⁺ cells from RUES1 and 43.6%–62.1% from the PPMS-iPSC lines. Additionally, we found that the O4⁺ fraction contained a subpopulation of cells double positive with PDGFR α (Figure 3J). O4⁺ cells could be easily purified by fluorescence-activated cell sorting (FACS), frozen, and thawed without losing their morphology (Figure S4D).

PPMS-Derived Late OPCs Myelinate Axons in the Mouse Brain

To verify that OPCs obtained through our protocol were functionally myelinogenic, we injected d75 FACS-purified O4⁺ cells into the forebrain of neonatal, immunocompromised shiverer mice (10⁵ cells/animal; Figure S4A). The injected cells were depleted of any contaminant iPSCs, as shown by flow-cytometry analysis of the pluripotency markers SSEA4 and TRA-1-60 (Figure S4B). However, we still purified our cultures before in vivo transplantation to retain the potential for translation to clinical studies. Cells were frozen, thawed, and allowed to recover for 24–48 hr before transplantation (Figure S4C). Animals were sacrificed at 12–16 weeks, at which point human hNA⁺ cells were distributed throughout the corpus callosum and forebrain white matter. The density of hNA⁺ cells in the corpus callosum was 34,400 \pm 3,090 cells/mm³ at 12 weeks and approximately double that by 16 weeks. We did not observe the presence of cell clusters or overt tumorigenesis, and the proliferative fraction of engrafted hNA⁺ cells was 17% at 12 weeks and decreased to only 8% Ki67⁺ at 16 weeks when only 5% of cells were PCNA⁺ (Figure 4H). Importantly, more than 80% of hNA⁺ cells in the corpus callosum coexpressed OLIG2 protein, suggesting that the engrafted cells were restricted to the oligodendrocyte lineage (Figure 4I). Furthermore, human MBP⁺ oligodendrocytes were found diffusely throughout engrafted corpus

callosum at 12 and 16 weeks (Figure 4A). At 16 weeks, 31% \pm 3% of host mouse axons were ensheathed within the engrafted mouse corpus callosum (Figure 4B).

We then asked whether PPMS-derived OPCs could form compact myelin. Transmission electron microscopy on 16-week-old corpus callosum revealed mature compact myelin with the presence of alternating major dense and intraperiod lines (Figures 4C and 4D), whereas uninjected shiverer/*rag2* mice possessed thin and loosely wrapped myelin (data not shown). Likewise, the thickness of myelin ensheathment, as assessed by g-ratio measurement, reflected a restoration of normal myelin in several callosal axons.

At 12 weeks, transplanted cells remained as NG2⁺ OPCs in the corpus callosum (Figure 4E), and by 16 weeks they started to migrate to the overlying cerebral cortex (Figure 4F). Very few O4-sorted cells underwent differentiation as hGFAP⁺ astrocytes and the majority of hGFAP⁺ cells were localized to the subventricular zone and around the ventricles (Figure 4G), suggesting that the local environment may induce astrocytic differentiation in these regions. Similarly, hNESTIN-expressing cells were rarely found in the corpus callosum and likewise concentrated in the subventricular zone (data not shown). Importantly, β III-TUBULIN⁺ neurons were not detected in any of the engrafted animals. Taken together, our data demonstrate that PPMS-derived, O4-sorted cells were capable of achieving mature oligodendrocyte differentiation in vivo and forming dense compact myelin resembling normal myelin in the brain.

DISCUSSION

In this work, using a fast and highly reproducible protocol, we demonstrated efficient in vivo myelination of neurons by iPSC-derived OPCs from PPMS patients. A previous report on MS-derived iPSCs showed that oligodendrocytes could be differentiated in vitro from an integrating, retrovirally reprogrammed iPSC line from one 35-year-old RRMS patient (Song et al., 2012); here, we generated four integration-free iPSC lines from PPMS patients of both sexes and with ages ranging from 50 to 62 years.

Since most protocols for oligodendrocyte differentiation have been optimized using only one or two hESC lines and their reproducibility with iPSC lines is controversial (Alsanie et al., 2013), we tested our protocol with two hESC and four hiPSC lines derived from PPMS patients. Previous

higher ($\times 64$; L) magnification, and MAP2⁺ and GFAP⁺ cells in oligodendrocyte cultures (M). PSC, pluripotent stem cell; NSC, neural stem cell; OPC, oligodendrocyte progenitor cell; OL, oligodendrocyte; pO/L, poly-L-ornithine/laminin.

Scale bars represent 500 μ m (B and K), 2 mm (C), and 200 μ m (D–F, H–J, and M). See also Figure S2 for proliferation assessment and quantification of MBP⁺ OLs and MAP2⁺ and GFAP⁺ cells.

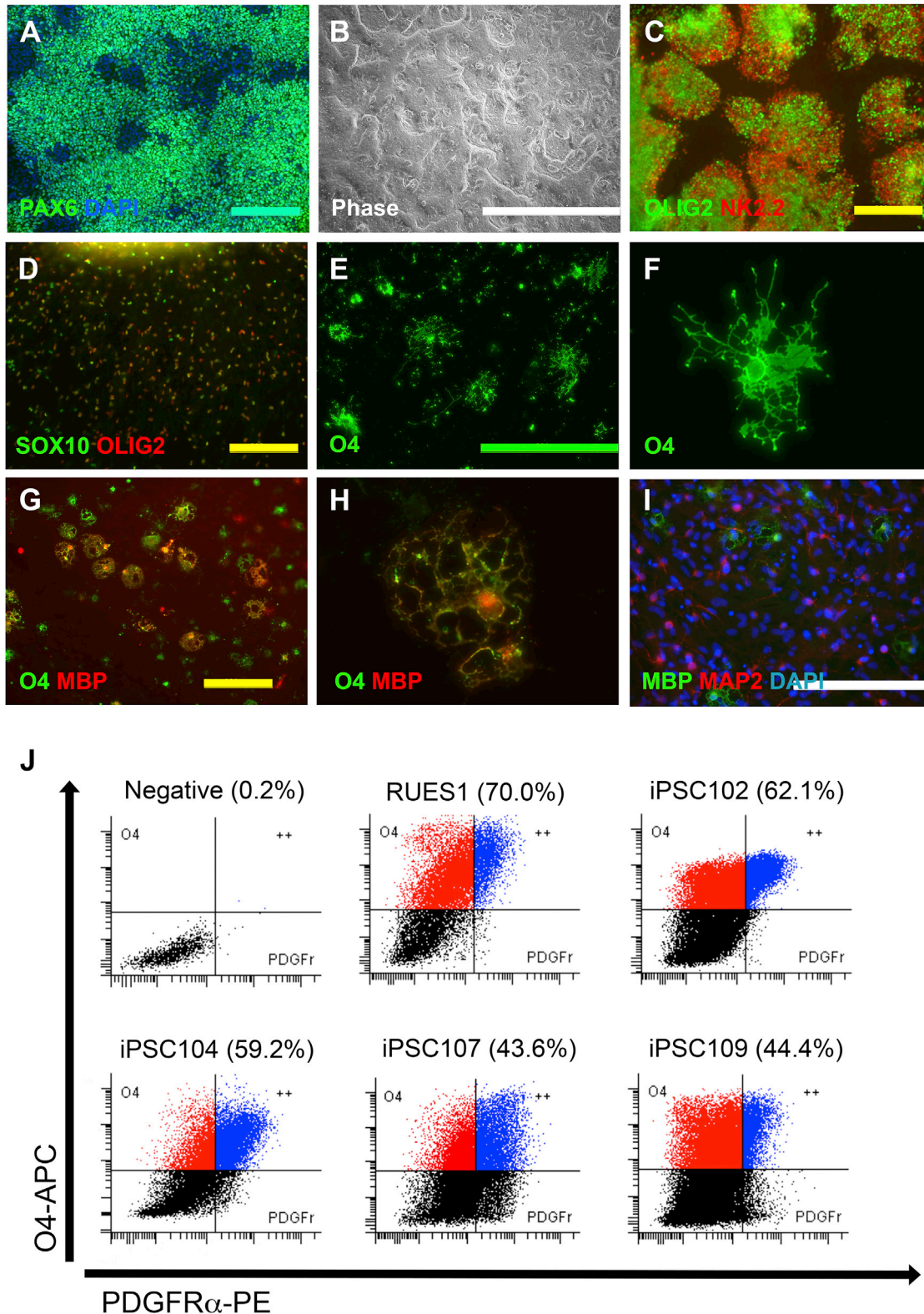


Figure 3. PPMS iPSCs Generate OPCs and Mature Oligodendrocytes In Vitro

(A–I) Sequential steps of in vitro oligodendrocyte differentiation of PPMS iPSCs, showing PAX6⁺ cells at day 8 (A), multilayered structures in phase contrast at day 12 (B), OLIG2⁺ and NKX2.2⁺ cells at day 12 (C), SOX10⁺OLIG2⁺ early OPCs (D), live imaging of O4⁺ late OPCs at day 12 (E–F), and mature oligodendrocytes (G–I) (legend continued on next page)



Stem Cell Reports

iPSC-Derived Oligodendrocytes from MS Patients

work has elegantly shown that iPSC-derived OPCs from healthy controls were able to rescue a mouse model of hypomyelination, although differentiation to the O4 stage was rather inefficient and required more than 120 days (Wang et al., 2013). We provide an improved differentiation protocol and further proof that patient-specific iPSC lines can be successfully used to generate oligodendrocytes. We obtained 44%–70% O4⁺ cells in all lines after 75 days of differentiation, compared with the minimum of 120 days required according to previous reports (Wang et al., 2013; Stacpoole et al., 2013). There are several critical differences between our approach and previously published protocols. First, we began neural induction with dual SMAD inhibition in adherent as opposed to suspension cultures (Nistor et al., 2005; Hu et al., 2009b; Wang et al., 2013). Using this approach, we started with only 10,000 cells/cm² of iPSCs at day 0 and achieved a great expansion of neural progenitors, ultimately generating an abundance of human OPCs. The use of RA and SHH as caudalizing and ventralizing patterning agents recapitulates the signals that are present around the pMN domain of the spinal cord, from which motor neurons and oligodendrocytes are believed to arise (Hu et al., 2009a). The high efficiency in the generation of OLIG2⁺ cells at d12 can be explained by the synergistic effect of activin/nodal receptor kinase inhibition, BMP4 inhibition, and RA and SHH signaling (Patani et al., 2011; Miller et al., 2004). The optimal concentration of RA in our hands is 100 times less than the concentration commonly used by other groups (Nistor et al., 2005; Izrael et al., 2007; Gil et al., 2009; Hu et al., 2009b). Surprisingly, induction with RA alone (without exogenous SHH) generated a large population of OLIG2⁺ cells. While the combination of RA and fibroblast growth factor (FGF) signaling is known to promote OLIG2 expression during chicken development and has been used for in vitro differentiation of both hESCs and hiPSCs (Novitsch et al., 2003; Nistor et al., 2005; Pouya et al., 2011), we achieved OLIG2 induction in the absence of any exogenous FGF in our culture conditions. We show that RA, synergistically with the dual inhibition of SMAD proteins, upregulates OLIG2 (Figure S1C), possibly by stimulating the endogenous expression of SHH (Figure S1A). We confirmed that SAG is an efficient replacement for SHH and indeed showed superior efficacy in our hands (Stacpoole et al., 2013). The addition of HGF to the medium, although not essential, appeared to slightly improve the differentiation efficiency (data not

shown; Hu et al., 2009c). Finally, the transition from adherent cultures to spheres proved to be a critical step to enrich the OLIG2⁺ population and possibly restrict differentiation to the oligodendrocyte lineage.

In human development, OPCs are characterized by PDGFR α and NG2 expression, followed by expression of O4 (Jakovcevski et al., 2009). Under our culture conditions, by day 75, most of the O4⁺ cells had lost PDGFR α , but retained NG2 expression. At this stage, we did not observe any residual pluripotent cells in culture. Our study differs from recent work in that our iPSC lines were derived from PPMS patients and the cells used for in vivo transplantation were sorted using the late-OPC marker O4 to maximally restrict the differentiation potential. Despite these differences, the PPMS-derived, O4⁺-sorted OPCs exhibited a similar engraftment efficiency, mitotic fraction, and proportion of host ensheathed axons while generating fewer GFAP⁺ astrocytes compared with the unsorted iPSC-derived OPCs reported previously. Taken together, our data suggest that PPMS-derived OPCs performed in vivo at least as efficiently as healthy iPSC-derived cells (Wang et al., 2013).

These proof-of-principle experiments establish that our OPC induction protocol can generate myelinogenic oligodendrocytes from patient samples and may be useful for the development of autologous cell-replacement therapies for MS in the future.

iPSC technology is also emerging as a tool for developing new drugs and gaining insight into disease pathogenesis (Han et al., 2011). Our differentiation protocol will aid the development of high-throughput in vitro screens for compounds that promote myelination (Lee et al., 2013). Furthermore, the PPMS iPSC lines described here provide an additional resource for investigating the process of neurodegeneration in MS. Future studies comparing PPMS iPSCs and appropriate healthy control iPSC lines will be needed to shed light on the potential intrinsic differences among patient-derived oligodendrocytes.

EXPERIMENTAL PROCEDURES

Subjects

Skin biopsies were obtained from deidentified PPMS patients at the Tisch Multiple Sclerosis Research Center of New York, upon institutional review board approval (BRANY) and receipt of informed consent. All four patients were diagnosed with PPMS according to the standard diagnostic criteria. All patients were Caucasian.

73 (E), a cropped image of O4⁺ cells to highlight the ramified processes (F), MBP⁺ mature oligodendrocytes at low (G) and higher ($\times 64$; H) magnification, and MAP2⁺ cells in the oligodendrocyte cultures (I). (J) Quantification of O4⁺ cells after 75 days of differentiation from RUES1 and PPMS iPSCs via FACS analysis. Gates are based on secondary Ab-APC only for O4 staining and PE-conjugated isotype control for PDGFR α staining (negative). Total O4⁺ cells (including O4 single-positive and O4/PDGFR α double-positive cells) are shown in brackets. Scale bars represent 200 μ m (A, C–E, G, and I) and 2 mm (B). See Figure S3 for characterization of PPMS-iPSC lines.

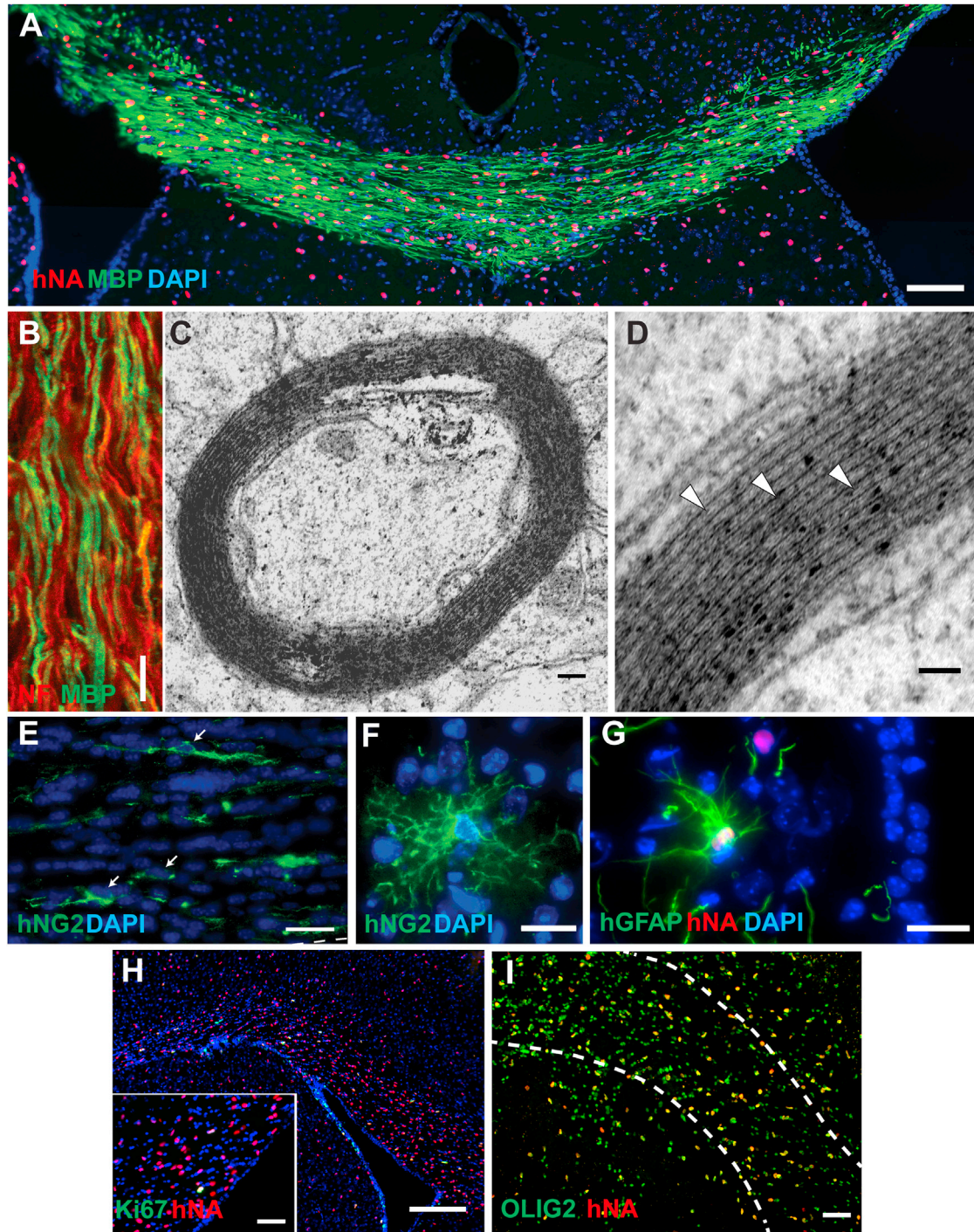


Figure 4. PPMS-Derived OPCs Engraft and Differentiate to Myelinogenic Oligodendrocytes In Vivo

(A) PPMS-iPSC-derived $O4^+$ OPCs (10^5) were transplanted into neonatal shiverer/*rag2* mice. At 16 weeks, MBP⁺ oligodendrocytes are widely distributed throughout the corpus callosum.

(B) Confocal image showing colocalization of mouse axons and MBP⁺ human oligodendrocytes.

(C and D) Electron micrographs of myelinated axons exhibiting characteristic compact myelin with alternating major dense (arrowheads) and intraperiod lines.

(E) Human cells retain progenitor characteristics, expressing a human specific-NG2 antigen (individual cells marked by arrows; 12 weeks).

(F) At 16 weeks, individual NG2 cells have begun to migrate into the overlying cerebral cortex.

(legend continued on next page)



Stem Cell Reports

iPSC-Derived Oligodendrocytes from MS Patients

Two patients were male (56 and 61 years old) and two were female (62 and 50 years old).

Cell Lines

Three hESC lines and four hiPSC lines were used for the study. RUES1 and HUES 45 are both NIH-approved hESC lines. The OLIG2-GFP reporter line is derived from the BG01 hESC line and was a gift from Dr. Ying Liu (University of Texas Health Science Center at Houston). Four iPSC lines were derived in our laboratory from skin biopsies of PPMS patients through the mRNA/miRNA method (StemGent).

Oligodendrocyte Differentiation Protocol

hESCs and hiPSCs were induced to neural differentiation through dual SMAD inhibition together with 100 nM all-*trans* RA. At day 8, SAG (1 μ M) was added to the medium, and at day 12, adherent cells were lifted and seeded in low-attachment plates to favor sphere aggregation. Spheres were cultured in the presence of RA and SAG. At day 30, spheres were plated into poly-L-ornithine/laminin-coated dishes and cells were allowed to migrate out of the sphere. At this stage, PDGF medium was used to promote OPC formation, and from day 75 onward, glial medium was used to drive oligodendrocyte maturation. For the qRT-PCR primer sequences and media compositions used, see [Tables S1](#) and [S2](#), respectively.

Transplantation into Shiverer \times *Rag2*^{-/-} Mice

All experiments using shiverer/*rag2* mice (a gift from Dr. Steven A. Goldman, University of Rochester; [Windrem et al., 2008](#)) were performed according to protocols approved by the University at Buffalo Institutional Animal Care and Use Committee. Injections were performed as previously described ([Sim et al., 2011](#)) and the animals were sacrificed 12–16 weeks later. Cryopreserved coronal sections were cut and immunohistochemistry was performed as described previously ([Sim et al., 2011](#)). For transmission electron microscopy, tissue was processed as described previously ([Sim et al., 2002](#)). For a list of the primary antibodies used, see [Table S3](#).

SUPPLEMENTAL INFORMATION

Supplemental Information includes Supplemental Experimental Procedures, four figures, and three tables and can be found with this article online at <http://dx.doi.org/10.1016/j.stemcr.2014.06.012>.

ACKNOWLEDGMENTS

We thank Drs. Dieter Egli and Haiqing Hua for the teratoma study and Dr. Ana Sevilla and Chris Woodard for the nanostring analysis. This work was supported by an NYSCF-Helmsley Early Career Investigator Award, The New York Stem Cell Foundation, and The Leona M. and Harry B. Helmsley Charitable Trust. *In vivo*

studies were supported by the Empire State Stem Cell Fund through the New York State Department of Health (contract C028108 to F.J.S.).

Received: January 6, 2014

Revised: June 23, 2014

Accepted: June 24, 2014

Published: July 24, 2014

REFERENCES

- Alsanie, W.F., Niclis, J.C., and Petratos, S. (2013). Human embryonic stem cell-derived oligodendrocytes: protocols and perspectives. *Stem Cells Dev.* *22*, 2459–2476.
- Antel, J., Antel, S., Caramanos, Z., Arnold, D.L., and Kuhlmann, T. (2012). Primary progressive multiple sclerosis: part of the MS disease spectrum or separate disease entity? *Acta Neuropathol.* *123*, 627–638.
- Chambers, S.M., Fasano, C.A., Papapetrou, E.P., Tomishima, M., Sadelain, M., and Studer, L. (2009). Highly efficient neural conversion of human ES and iPS cells by dual inhibition of SMAD signaling. *Nat. Biotechnol.* *27*, 275–280.
- Gil, J.E., Woo, D.H., Shim, J.H., Kim, S.E., You, H.J., Park, S.H., Paek, S.H., Kim, S.K., and Kim, J.H. (2009). Vitronectin promotes oligodendrocyte differentiation during neurogenesis of human embryonic stem cells. *FEBS Lett.* *583*, 561–567.
- Goldman, S.A., Nedergaard, M., and Windrem, M.S. (2012). Glial progenitor cell-based treatment and modeling of neurological disease. *Science* *338*, 491–495.
- Han, S.S.W., Williams, L.A., and Eggan, K.C. (2011). Constructing and deconstructing stem cell models of neurological disease. *Neuron* *70*, 626–644.
- Hauser, S.L., Chan, J.R., and Oksenberg, J.R. (2013). Multiple sclerosis: Prospects and promise. *Ann. Neurol.* *74*, 317–327.
- Hu, B.Y., Du, Z.W., Li, X.J., Ayala, M., and Zhang, S.C. (2009a). Human oligodendrocytes from embryonic stem cells: conserved SHH signaling networks and divergent FGF effects. *Development* *136*, 1443–1452.
- Hu, B.Y., Du, Z.W., and Zhang, S.C. (2009b). Differentiation of human oligodendrocytes from pluripotent stem cells. *Nat. Protoc.* *4*, 1614–1622.
- Hu, Z., Li, T., Zhang, X., and Chen, Y. (2009c). Hepatocyte growth factor enhances the generation of high-purity oligodendrocytes from human embryonic stem cells. *Differentiation* *78*, 177–184.
- Izrael, M., Zhang, P., Kaufman, R., Shinder, V., Ella, R., Amit, M., Itskovitz-Eldor, J., Chebath, J., and Revel, M. (2007). Human oligodendrocytes derived from embryonic stem cells: effect of noggin on phenotypic differentiation *in vitro* and on myelination *in vivo*. *Mol. Cell. Neurosci.* *34*, 310–323.

(G) Only a few hGFAP⁺ astrocytes are found in proximity to the lateral ventricle.

(H) Very few of the engrafted human cells are still proliferative 16 weeks after transplantation. Insert is a higher-magnification image.

(I) OLIG2⁺/hNA⁺ progenitor cells 16 weeks after transplantation. hNA, human nuclear antigen; NF, neurofilament.

Scale bars represent 100 μ m (A), 10 μ m (B), 100 nm (C), 50 nm (D), 25 μ m (E–G), 200 μ m (H and I), and 50 μ m (inset in H). See also [Figure S4](#) for details on cells immediately before transplantation.



- Jakovcevski, I., Filipovic, R., Mo, Z., Rakic, S., and Zecevic, N. (2009). Oligodendrocyte development and the onset of myelination in the human fetal brain. *Front Neuroanat* 3, 5.
- Lee, S., Chong, S.Y., Tuck, S.J., Corey, J.M., and Chan, J.R. (2013). A rapid and reproducible assay for modeling myelination by oligodendrocytes using engineered nanofibers. *Nat. Protoc.* 8, 771–782.
- Liu, Y., Jiang, P., and Deng, W. (2011). OLIG gene targeting in human pluripotent stem cells for motor neuron and oligodendrocyte differentiation. *Nat. Protoc.* 6, 640–655.
- Miller, R.H., Dinsio, K., Wang, R., Geertman, R., Maier, C.E., and Hall, A.K. (2004). Patterning of spinal cord oligodendrocyte development by dorsally derived BMP4. *J. Neurosci. Res.* 76, 9–19.
- Nistor, G.I., Totoiu, M.O., Haque, N., Carpenter, M.K., and Keirstead, H.S. (2005). Human embryonic stem cells differentiate into oligodendrocytes in high purity and myelinate after spinal cord transplantation. *Glia* 49, 385–396.
- Novitsch, B.G., Wichterle, H., Jessell, T.M., and Sockanathan, S. (2003). A requirement for retinoic acid-mediated transcriptional activation in ventral neural patterning and motor neuron specification. *Neuron* 40, 81–95.
- Patani, R., Hollins, A.J., Wishart, T.M., Puddifoot, C.A., Alvarez, S., de Lera, A.R., Wyllie, D.J., Compston, D.A., Pedersen, R.A., Gillingwater, T.H., et al. (2011). Retinoid-independent motor neurogenesis from human embryonic stem cells reveals a medial columnar ground state. *Nat. Commun.* 2, 214.
- Pouya, A., Satarian, L., Kiani, S., Javan, M., and Baharvand, H. (2011). Human induced pluripotent stem cells differentiation into oligodendrocyte progenitors and transplantation in a rat model of optic chiasm demyelination. *PLoS One* 6, e27925.
- Rice, C.M., Cottrell, D., Wilkins, A., and Scolding, N.J. (2013). Primary progressive multiple sclerosis: progress and challenges. *J. Neurol. Neurosurg. Psychiatry* 84, 1100–1106.
- Sim, F.J., Zhao, C., Li, W.W., Lakatos, A., and Franklin, R.J. (2002). Expression of the POU-domain transcription factors SCIP/Oct-6 and Brn-2 is associated with Schwann cell but not oligodendrocyte remyelination of the CNS. *Mol. Cell. Neurosci.* 20, 669–682.
- Sim, F.J., McClain, C.R., Schanz, S.J., Protack, T.L., Windrem, M.S., and Goldman, S.A. (2011). CD140a identifies a population of highly myelinogenic, migration-competent and efficiently engrafting human oligodendrocyte progenitor cells. *Nat. Biotechnol.* 29, 934–941.
- Song, B., Sun, G., Herszfeld, D., Sylvain, A., Campanale, N.V., Hirst, C.E., Caine, S., Parkinson, H.C., Tonta, M.A., Coleman, H.A., et al. (2012). Neural differentiation of patient specific iPSCs as a novel approach to study the pathophysiology of multiple sclerosis. *Stem Cell Res. (Amst.)* 8, 259–273.
- Stacpoole, S.R.L., Spitzer, S., Bilican, B., Compston, A., Karadottir, R., Chandran, S., and Franklin, R.J.M. (2013). High yields of oligodendrocyte lineage cells from human embryonic stem cells at physiological oxygen tensions for evaluation of translational biology. *Stem Cell Rep.* 1, 437–450.
- Wang, S., Bates, J., Li, X., Schanz, S., Chandler-Militello, D., Levine, C., Maherali, N., Studer, L., Hochedlinger, K., Windrem, M., and Goldman, S.A. (2013). Human iPSC-derived oligodendrocyte progenitor cells can myelinate and rescue a mouse model of congenital hypomyelination. *Cell Stem Cell* 12, 252–264.
- Warren, L., Manos, P.D., Ahfeldt, T., Loh, Y.H., Li, H., Lau, F., Ebina, W., Mandal, P.K., Smith, Z.D., Meissner, A., et al. (2010). Highly efficient reprogramming to pluripotency and directed differentiation of human cells with synthetic modified mRNA. *Cell Stem Cell* 7, 618–630.
- Windrem, M.S., Schanz, S.J., Guo, M., Tian, G.F., Washco, V., Stanwood, N., Rasband, M., Roy, N.S., Nedergaard, M., Havton, L.A., et al. (2008). Neonatal chimerization with human glial progenitor cells can both remyelinate and rescue the otherwise lethally hypomyelinated shiverer mouse. *Cell Stem Cell* 2, 553–565.
- Yamada, M., Johannesson, B., Sagi, I., Burnett, L.C., Kort, D.H., Prosser, R.W., Paull, D., Nestor, M.W., Freeby, M., Greenberg, E., et al. (2014). Human oocytes reprogram adult somatic nuclei of a type 1 diabetic to diploid pluripotent stem cells. *Nature* 510, 533–536. <http://dx.doi.org/10.1038/nature13287>.

Stem Cell Reports, Volume 3

Supplemental Information

**Efficient Generation of Myelinating Oligodendrocytes
from Primary Progressive Multiple Sclerosis
Patients by Induced Pluripotent Stem Cells**

**Panagiotis Douvaras, Jing Wang, Matthew Zimmer, Stephanie Hanchuk, Melanie
A. O'Bara, Saud Sadiq, Fraser J. Sim, James Goldman, and Valentina Fossati**

Figure S1

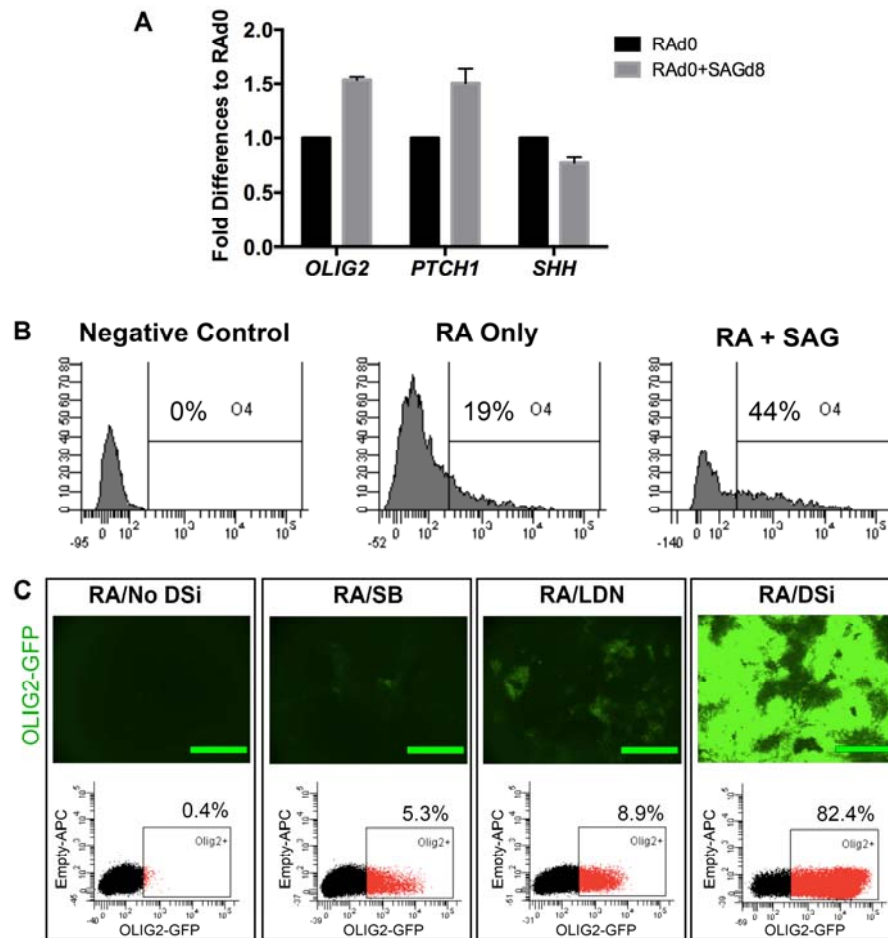


Figure S1. SHH and dual SMAD inhibition requirements for OLIG2⁺ progenitors, Related to Figure 1. (A) mRNA levels for *OLIG2*, *PTCH1* and *SHH* at day 14 of differentiation between cultures with RA from d0 and SHH/SAG from d8 compared to cells that were exposed only to RA from d0. Endogenous *SHH* levels are higher in the samples that were not exposed to SHH/SAG. Error bars are SEM (N=3 independent experiments). **(B)** FACS-analysis for O4⁺ cells at day 75 of differentiation between cells that were exposed to RA only or RA and SAG in the first 12 days of differentiation. A 56% decrease in the O4⁺ population was observed in the cells that were not provided with SAG in the initial steps of differentiation. Negative Control: APC-conjugated secondary antibody only. **(C)** Live imaging and FACS-analysis at day 14 of differentiation under different SMAD inhibitors. A substantial population of GFP⁺ cells is present only under the dual inhibition of SMAD proteins, indicating a synergistic effect between RA and the dual inhibition of SMAD. DSi: Dual SMAD inhibition; SB: SB431542; LDN: LDN189193. Scale bars are 500µm.

Figure S2

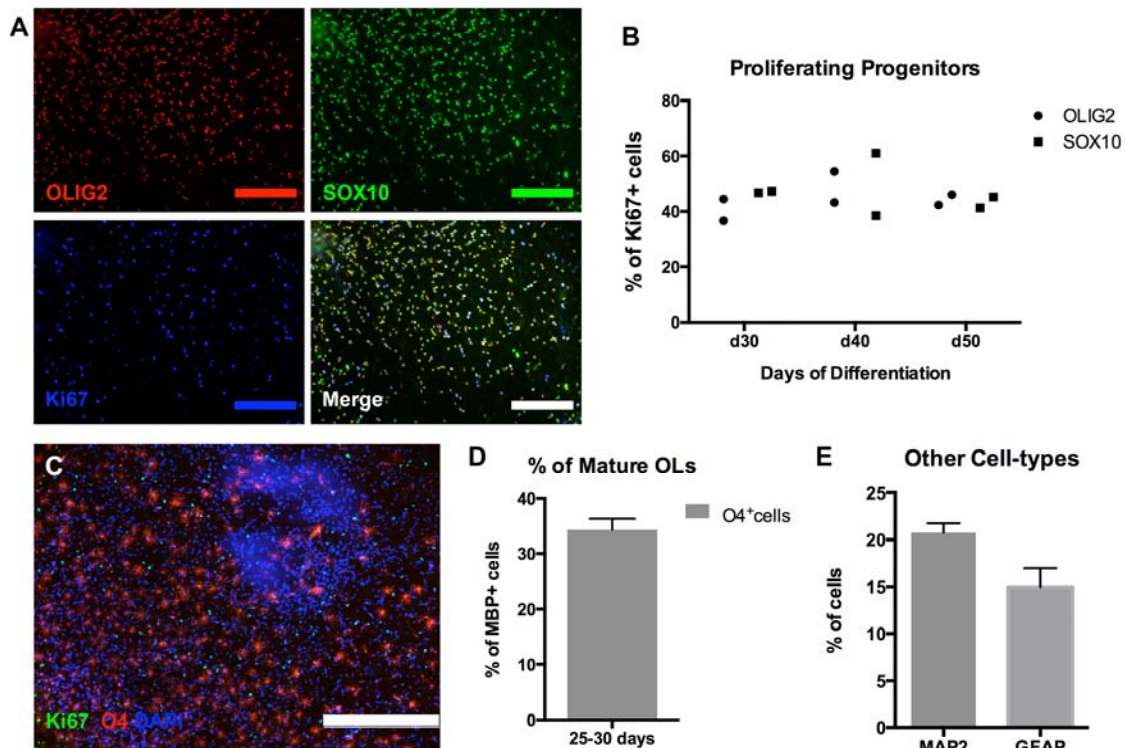


Figure S2. Proliferative oligodendrocytes and other neural cell-types, Related to Figure 2. (A) Representative immunofluorescence staining at d50 of differentiation for OLIG2, SOX10 and Ki67. There is an almost complete co-localization between OLIG2 and SOX10. (B) Dot plot showing the temporal quantification of proliferating (Ki67⁺) OLIG2⁺ and SOX10⁺ progenitors between d30 and d50 of differentiation in two independent experiments (N=2). (C) Immunofluorescence image of a culture at d73 showing a large number of highly ramified O4⁺ cells. Hardly any O4⁺ cell is co-expressing Ki67. (D) Percentage of O4⁺ cells that co-express MBP in cultures 25 – 30 days after growth-factor removal (Glial medium). Error bar is SEM (N=4 independent experiments). (E) Graph showing the percentage of MAP2⁺ neurons and GFAP⁺ astrocytes out of the total number of cells in three independent experiments at d78 – d88 of differentiation. Error bars are SEM (N=3). Scale bars are 200 μ m (A) and 500 μ m (C).

Figure S3

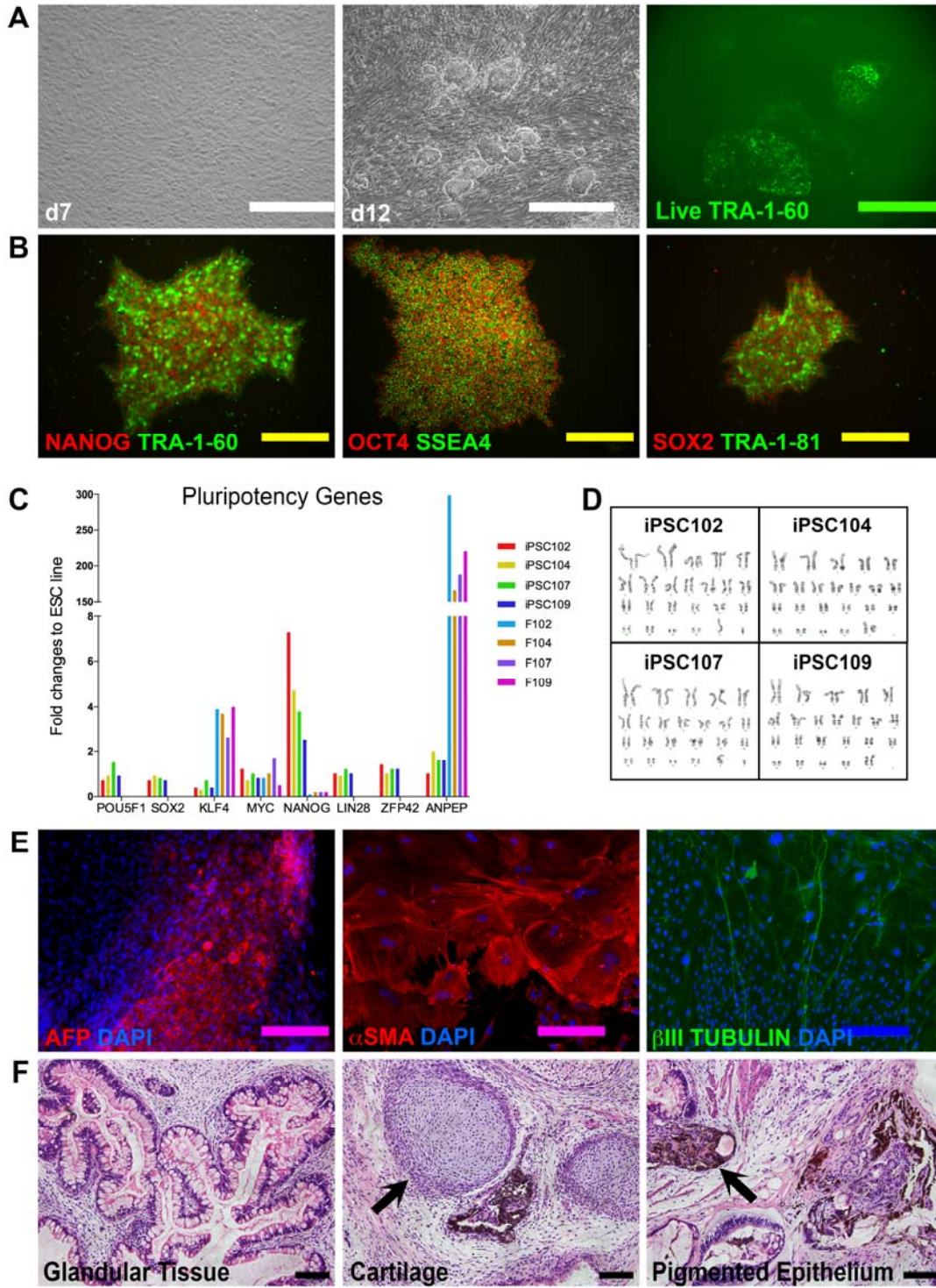


Figure S3. Generation and characterization of PPMS iPSC lines, Related to Figure 3. (A) mRNA/miRNA reprogramming of PPMS lines showing representative skin fibroblasts at day 7, iPSC-like colonies evident at day12 and TRA-1-60⁺ colonies at day15 of reprogramming. (B) Immunofluorescence of PPMS-iPSC line 102 for pluripotency markers. (C) Pluripotency gene expression of undifferentiated PPMS-iPSCs and parental fibroblasts, relative to a hESC line. *ANPEP* gene is specific for fibroblasts. (D) Cytogenetic analysis of all PPMS-iPSC lines shows a normal karyotype. (E) Immunofluorescence after *in vitro* spontaneous differentiation through embryoid bodies for endodermal marker AFP, mesodermal marker α SMA and ectodermal marker β III-TUBULIN. Nuclei are stained with DAPI. (F) H&E stained sections of *in vivo* teratoma formation after injection of PPMS iPSCs into immunodeficient mice show representative structures from glandular tissue (endoderm), cartilage (mesoderm) and pigmented epithelium (ectoderm). Scale bars are 500 μ m (A), 200 μ m (B, E) and 100 μ m (F).

Figure S4

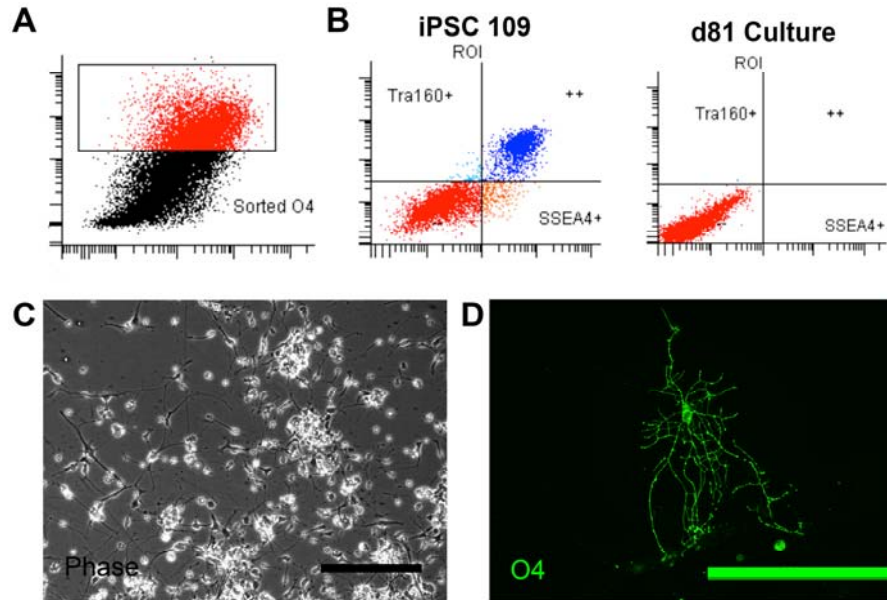


Figure S4. Characterization of cells before transplantation for the *in vivo* studies, Related to Figure 4. (A) FACS plot showing the more stringent gate used for sorting O4⁺ cells before isolation and cryopreservation for the *in vivo* transplantations. **(B)** FACS plots showing pluripotency markers in an iPSC line grown on MEFs and the lack of the same markers in cells at d81 of differentiation. **(C)** A brightfield image of O4⁺ sorted cells plated after cryopreservation during the recovery period (24 hours). **(D)** Live O4 staining in sorted OPCs showing the retention of O4 antigen and the proper ramified morphology.

Table S1. Sequences of the primers used for qRT-PCR, Related to Experimental Procedures.

Target gene	Forward primer	Reverse primer
PAX6	TTTGCCCGAGAAAGACTAGC	CATTTGGCCCTTCGATTAGA
OLIG2	TGCGCAAGCTTTCCAAGA T	CAGCGAGTTGGT GAGCATGA
NKX2.2	GACAACTGGTGGCAGATTTTCGCTT	AGCCACAAAGAAAGGAGTTGGACC
PTCH1	ATCTGCACCGGCCAGCTACT	CCACCGCGAAGGCCCAAATA
SHH	AAACACCGGAGCGGACAGGC	GGTCGCGGTCAGACGTGGTG

Table S2. Detailed composition of culturing media, Related to Experimental Procedures.

Media	Components	Provider	Final Conc.
N₂ Medium	<u>DMEM/F12</u>	Life Technologies	
	Glutamax (100X)	Life Technologies	1X
	Non-Essential Aminoacids (100X)	Life Technologies	1X
	β-Mercaptoethanol (1000X)	Life Technologies	1X
	Penicillin-Streptomycin (100X)	Life Technologies	1X
	N ₂ Supplement (100X)	Life Technologies	1X
N₂B₂₇	<u>N₂ Medium</u>		
	B ₂₇ Supplement (50X)	Life Technologies	1X
PDGF Medium	<u>N₂ B₂₇ Medium</u>		
	PDGF	R&D Systems	10ng/ml
	IGF	R&D Systems	10ng/ml
	HGF	R&D Systems	5ng/ml
	NT3	Millipore	10ng/ml
	Insulin	Sigma	25µg/ml
	Biotin	Sigma	100ng/ml
	cAMP	Sigma	1µM
T3	Sigma	60ng/ml	
Glial Medium	<u>N₂ B₂₇ Medium</u>		
	Ascorbic Acid	Sigma	20µg/ml
	HEPES	Sigma	10mM
	Insulin	Sigma	25µg/ml
	Biotin	Sigma	100ng/ml
	cAMP	Sigma	1µM
T3	Sigma	60ng/ml	

Table S3. List of Primary Antibodies, Related to Experimental Procedures.

Antigen	Dilution	Host	Provider
OCT4	1:250	Rabbit	Stemgent
TRA-1-60	1:250	Mouse	EMD Millipore
SOX2	1:250	Rabbit	Stemgent
TRA-1-81	1:250	Mouse	EMD Millipore
NANOG	1:100	Rabbit	Cell Signaling
SSEA4	1:250	Mouse	Abcam
AFP	1:300	Rabbit	Dako
α SMA	1:300	Mouse	Sigma
β III \square TUBULIN	1:500	Chicken	Neuromics
TRA-1-60-488 (FACS)	1:100	Mouse	BD Biosciences
SSEA4-647 (FACS)	1:100	Mouse	BD Biosciences
PDGFR α -PE	1:5	Mouse	BD Biosciences
PAX6	1:250	Rabbit	Covance
OLIG2	1:500	Rabbit	EMD Millipore
NKX2.2	1:75	Mouse	DSHB
SOX10	1:100	Goat	R&D Systems
NG2	1:200	Mouse	BD Biosciences
O4	1:30	Mouse	J.G. laboratory
MBP	1:200	Rat	EMD Millipore
MAP2	1:5000	Chicken	Abcam
GFAP	1:750	Rabbit	Dako
Ki67 (<i>in vivo</i>)	1:250	Rabbit	EMD Millipore
hNA clone 235-1	1:100	Mouse	EMD Millipore
MBP (<i>in vivo</i>)	1:300	Rat	Abcam
GFAP (<i>in vivo</i>)	1:800	Mouse	Covance
NG2 (<i>in vivo</i>)	1:800	Mouse	EMD Millipore
SMI311 & SMI312 (mNeurofilament)	1:800	Mouse	Covance

Supplemental Experimental Procedures

hPSCs culture conditions

hESC and hiPSC lines were cultured and expanded with HUESM (HUMAN Embryonic Stem Medium) medium and 10 ng/ml bFGF (StemCell Technologies) onto mouse embryonic fibroblast (MEF) layer. For oligodendrocyte differentiation, cells were adapted to cultures onto matrigel-coated dishes and mTeSR1 medium (StemCell Technologies). HUESM is composed by Knockout-DMEM, 20% Knock-out serum, glutamax 2mM, NEAA 0.1mM, 1X P/S and β -mercaptoethanol 0.1mM all purchased from Life Technologies.

Derivation of skin fibroblasts from punch biopsies

Three mm skin biopsies were collected in Biopsy Collection Medium, consisting of RPMI 1460 (Gibco) and 1X Antibiotic-Antimycotic (Life Technologies). Biopsies were sliced into smaller pieces (<1mm) and plated onto a TC-treated 35mm dish for 5 minutes to dry and finally they were incubated in Biopsy Plating Medium, composed by Knockout DMEM, 2mM GlutaMax, 0.1mM NEAA, 0.1mM β -Mercaptoethanol, 10% Fetal Bovine Serum (FBS), 1X Penicillin-Streptomycin (P/S; all from Life Technologies) and 1% Nucleosides (Millipore), for 5 days or until the first fibroblasts grew out of the biopsy. Alternatively, biopsies were digested with 1000U/ml Collagenase 1A (Sigma) for 1.5 hours at 37°C, washed, collected and plated onto 1% gelatin-coated 35mm dish in Biopsy Plating Medium for 5 days. Fibroblasts were then expanded in Culture Medium, consisting of DMEM (Life Technologies), 2mM GlutaMax, 0.1mM NEAA, 0.1mM β -Mercaptoethanol, 10% FBS and 1X P/S changing medium every other day.

Reprogramming of skin fibroblasts

Skin fibroblasts at passage 3 to 5 were reprogrammed using the StemGent mRNA/miRNA kit, which results in the generation of integration-free, virus free human iPSCs, through modified RNAs for *OCT4*, *SOX2*, *KLF4*, *cMYC* and *LIN28*. The addition of a specific cluster of miRNA has been found to increase the efficiency of reprogramming (StemGent). Briefly, fibroblasts were plated onto Matrigel-coated 6-well or 12-well plates in a 5.5×10^3 cells/cm² density in Culture medium. The following day, medium was replaced with NuFF-conditioned Pluriton reprogramming medium containing B18R. Cells were transfected for 11 consecutive days using Stemfect as following: day 0 miRNA only, day1 to day3 mRNA cocktail only, d4 miRNA plus mRNA cocktail, day 5 to day 11 mRNA cocktail only. After day 11, visible colonies positively stained for live TRA-1-60 were picked and re-plated on MEFs with HUESM medium.

Teratoma assay

Experiments were performed according to a protocol approved by the Columbia Institutional Animal Care and Use Committee (IACUC).

iPSC colonies were dissociated using Collagenase (Sigma) for 15 minutes at 37°C, washed, collected and re-suspended in 200µl HUESM. Cells were then mixed with 200µl Matrigel™ (BD Biosciences) on ice and were injected subcutaneously into immunodeficient mice (Jackson Laboratory). Teratomas were allowed to grow for 9–12 weeks, isolated by dissection and fixed in 4% PFA overnight at 4°C. Fixed tissues were embedded in paraffin, sectioned at 10µm thickness and stained with hematoxylin and eosin (H&E).

Spontaneous differentiation *in vitro*

iPSCs were dissociated with Accutase (Life Technologies) for 5 minutes at 37°C and seeded into Ultra-Low attachment 6-well plates in HUESM without bFGF, changing media every other day. After 3 weeks of culture, EBs were plated onto 1% gelatin-coated TC-treated dishes for another 2 weeks. EBs and their outgrowth were fixed in 4% PFA for 8 minutes at RT and immunostained for the appropriate markers.

RNA isolation and qRT-PCR

RNA isolation was performed using the RNeasy Plus Mini Kit (Qiagen) with QIAshredder (Qiagen). Briefly, cells were pelleted, washed with PBS and re-suspended in lysis buffer. Samples were then stored at -80°C until processed further according to manufacturer's instructions. RNA was eluted in 30µl RNase free ddH₂O and quantified with a NanoDrop 8000 spectrophotometer (Thermo Scientific).

For qRT-PCR, cDNA was synthesized using the GoScript Reverse Transcription System (Promega) with 0.5µg of RNA and random primers. 20ng of cDNA were then loaded to a 96-well reaction plate together with 10µl GoTaq qPCR Master Mix and 1µl of each primer (10nM) in a 20µl reaction and the plate was ran in Stratagene Mx300P qPCR System (Agilent Technologies). For primer sequences see Table s1.

Nanostring analysis for pluripotency

RNA was isolated from undifferentiated iPSCs and hESC HUES45 as previously described. 100ng of RNA per sample were loaded for the hybridization with the specific Reporter Code Set and Capture Probe Set (Nanostring Technologies) according to manufacturer's instructions. Data were normalized to the following house keeping genes: *ACTB*, *POLR2A*, *ALAS1*. Data were expressed as fold changes to the expression of the hESC line (HUES45=1).

Karyotyping

All iPSC-lines were subjected to cytogenetic analysis by Cell Line Genetics to confirm a normal karyotype.

Detailed oligodendrocyte differentiation protocol

Cells were plated on Matrigel (Bd Biosciences) in a 10×10^3 cells/cm² density in mTeSR1 medium (StemCell Technologies) containing 10 μ M Rock Inhibitor (Y-27632; StemGent) for 24 hours. At the day of differentiation induction (d0), medium was switched to mTeSR Custom (StemCell Technologies), containing the small molecules SB431542 10 μ M (StemGent) and LDN193189 250nM (StemGent) as well as 100nM all-trans-retinoic acid (RA; Sigma). mTeSR Custom medium has the same composition as the commercially available mTeSR-1 medium but without 5 factors that sustain pluripotency, namely Lithium Chloride, GABA, Pipelicolic Acid, bFGF and TGF β 1 (Stem Cell Technologies). Media changes were performed daily until d8, when the media was switched to N₂ medium containing 100nM RA, 1 μ M SAG (Millipore) or 100ng/ml rhSHH (R&D system), changed daily. At d12, cells were detached using a cell-lifter and re-plated into Ultra-low attachment plates in N₂B₂₇ medium containing 1 μ M SAG, changing it every other day. At day 20, medium was switched to PDGF medium, and 2/3 media changes were performed every other day. At day 30, spheres were plated onto plates coated with poly-L-ornithine hydrobromide (50 μ g/ml; Sigma) and Laminin (20 μ g/ml; Life Technologies) in a 2 spheres/cm² density. This density was optimized to allow cells to migrate out from the sphere, proliferate and spread to the entire dish by the end of the protocol without the need for passaging. For terminal oligodendrocyte differentiation, cells from day 75 were cultured in Glial medium, changing 2/3 of the medium every 3 days. For a complete list of medium composition see Table s2.

Immunostaining

Cells were washed 3X in PBS-T (PBS containing 0.1% Triton-X100) for 10 minutes, incubated for 2 hours in blocking serum (PBS-T with 5% goat or donkey serum) and primary antibodies were applied overnight at 4°C (See Table s3). The next day, cells were washed 3X in PBS-T for 15 minutes, incubated with secondary antibodies for 2 hours at room-temperature (RT), washed 3X for 10 minutes in PBS-T, counterstained with DAPI for 15 minutes at RT and washed 2X in PBS. Alexa Fluor secondary antibodies, goat or donkey anti-mouse, rat, rabbit, goat and chicken 488, 555, 568, and 647 were used at 1:500 dilution (Invitrogen). Images were acquired using an Olympus IX71 inverted microscope, equipped with Olympus DP30BW black and white digital camera for fluorescence and DP72 digital color camera for H&E staining. Fluorescent colors were digitally

applied using the Olympus software DP Manager or with imageJ. For counting, at least three non-overlapping fields were imported to ImageJ, thresholded and scored manually.

Flow cytometry

Cells were enzymatically harvested by Accutase treatment for 25 min at 37°C to obtain a single cell suspension. Cells were then re-suspended in 100 µl of their respective medium containing the appropriate amount of either primary antibody or fluorescence-conjugated antibodies and were incubated on ice for 30 minutes shielded from light. When secondary antibodies were used, primary antibodies were washed with PBS and secondary antibodies were applied for 30 minutes on ice. Stained or GFP expressing cells were washed with PBS and sorted immediately on a 5 laser BD Biosciences ARIA-IIu™ Cell Sorter using the 100 µm ceramic nozzle, and 20 psi. DAPI was used for dead cell exclusion. Flow cytometry data were analyzed using BD FACSDiva™ software.

Transplantation into shiverer (*shi/shi*) x *Rag2*^{-/-} mice

FACS-sorted O4⁺ OPCs that have been previously cryopreserved were thawed and allowed to recover for 1-2 days prior to surgery by plating on pO/L dishes in PDGF Medium. Cells were prepared for injection by re-suspending cells at 1 x 10⁵ cells per µl. Pups were anesthetized using hypothermia and 5 x 10⁴ cells were injected in each site, bilaterally at a depth of 1.1mm into the corpus callosum of postnatal day 2-3 pups. Cells were injected through pulled glass pipettes, inserted directly through the skull into the presumptive target sites. Animals were sacrificed and perfused with saline followed by 4% paraformaldehyde at 12 or 16 weeks. Cryopreserved coronal sections of mouse forebrain (16 µm) were cut and sampled every 160 µm. Human cells were identified with mouse antihuman nuclei (hNA) and myelin basic protein-expressing oligodendrocytes were labeled with MBP. Human astrocytes and OPCs were stained with human-specific antibodies against hGFAP and hNG2 respectively. Mouse neurofilament (NF) was stained by 1:1 mixture of SMI311 and SMI312. Alexa Fluor secondary antibodies, goat anti-mouse 488, 594, and 647 were used at 1:500 dilution (Invitrogen). For EM, mice were killed under deep anesthesia by perfusion with 4% glutaraldehyde via the left ventricle. Brains were removed and postfixed overnight and 1.5-mm-thick blocks containing the corpus callosum were cut. Blocks were postfixed in osmium tetroxide at 4°C overnight, dehydrated through ascending ethanol washes, and embedded in TAAB resin (TAAB Laboratories, Aldermaston, UK). One-micrometer sections were cut, stained using toluidine blue, and examined by light microscopy. In addition, selected blocks were trimmed and examined by electron microscopy.